School of Chemistry and Chemical Engineering, Shanghai University of Engineering Science, Shanghai, China

Crystal structure, dissolution and hygroscopicity of a novel cocrystal hydrate of berberine hydrochloride with L(+)-lactic acid

Lili Wang, Shuyu Liu*, Ziyao Gao

Received June 23, 2020, accepted August 12, 2020

**Corresponding author: Shuyu Liu, School of Chemistry and Chemical Engineering, Shanghai University of Engineering Science, Shanghai 201620, China.*
Email: liushuyu1219@163.com

Pharmazie 75: 483-487 (2020) *doi: 10.1691/ph.2020.0079*

Berberine hydrochloride (BCl) is commercially used to treat diarrhea, diabetes, hyperlipidemia, and cancer. However, BCl suffers from solid state instability, low aqueous solubility, low dissolution rate, and poor bioavailability, which limit its potential application in clinical medicine. In this work, we report a novel cocrystal hydrate of BCl with L(+)-lactic acid (BCl-LA-H_2O), designed to improve its physicochemical properties, thus promoting its application in the pharmaceutical industry. As a result, the cocrystal strategy improved the solubility, dissolution, melting point, and hygroscopicity of BCl, which indicated that the BCl-LA-H_2O can be used as a better solid form.

1. Introduction

It is well known that the active pharmaceutical ingredient (API) is very important in the process of the drug development (Shimpi et al. 2018). The efficacy of a drug is often dependent on the bioavailability of the APIs (Childs et al. 2004), and different solid states of API display different physicochemical properties that can profoundly affect the bioavailability of a resulting dosage form (Childs et al. 2013; Kobayashi et al. 2000; Jung et al. 2010). Therefore, many methods have been proposed to change the solid states of APIs to improve their physicochemical properties, including hydrates, polymorphs, solvates, amorphous forms, salts, and cocrystals (Chen et al. 2016). Recently, more and more pharmaceutical researchers are drawing their interests on the cocrystal technique dute to its huge potential market value in the research process of drug (Du et al. 2017). More specifically, in addition to providing the opportunity to increase the quantities and types of solid drugs (Thakuria et al. 2013), crystallization can also provide a way to modify the physicochemical properties of the APIs without changing the chemical structures and the inherent biological activities (Qiao et al. 2011; Desiraju 2013; Bavishi and Borkhataria 2016).

Berberine hydrochloride (BCl, molecular weight (MW)=371.82) is an isoquinoline alkaloid and one of the main components in coptidis rhizoma. Due to its antibacterial and antisecretory properties, it is commercially used to treat diarrhea caused by bacteria (Su et al. 2019). Many studies have shown that berberine is a potential drug for the treatment of diabetes, hyperlipidemia and cancer (Jin et al. 2015; Sun et al. 2009; Liu et al. 2016). One of the key factors limiting the clinical application of BCl is phase transition due to its remarkable hygroscopicity under ordinary storage conditions (Lu et al. 2019; Xu et al. 2019). It exhibited solid state instability since it could undergo solid state transformations among anhydrate, dehydrate and tetrahydrate depending on relative humidity (Tong et al. 2010). Consequently, commercial BCl is usually a mixture of the dihydrate and tetrahydrate forms. In addition, BCl has the disadvantages of low aqueous solubility, low dissolution, and poor bioavailability (Pingali et al. 2015; Zhu et al. 2013). Therefore, in recent years, we are committed to gradually solving these problems via crystal engineering to design and synthesize new cocrystals of BCl to obtain the best solid state of clinical medicine of BCl.

In the present study, we report a novel crystal form of BCl with L (+)-lactic acid (LA) (Fig. 1) was prepared by liquid-assisted grinding method. And it was characterized by solid-state material characterization techniques, which were powder X-ray diffraction, fourier transform infrared spectroscopy, and thermal analysis. And the structure of the novel cocrystal was determined by single crystal X-ray diffraction analysis. In addition, its solubility, dissolution, and dynamic vapor adsorption were evaluated. All of these results showed that the cocrystal exhibited good physicochemical properties compared with BCl·$2H_2O$. The main results of the present investigation confirm that the cocrystal have unique properties which may create high commercial value.

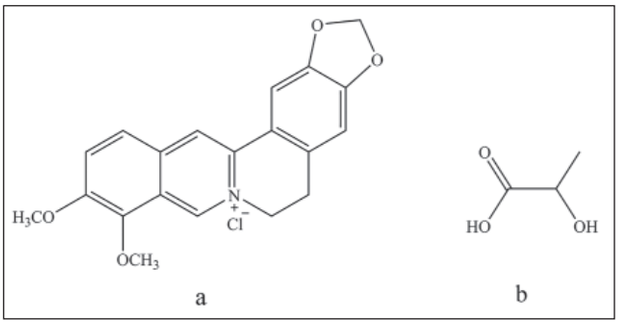

Fig. 1: The chemical structures of (a) berberine chloride and (b) L (+)-lactic acid.

2. Investigations, results and discussion

2.1. Crystal structures analysis

The crystallographic data and details of refinement were listed in Table 1 and 2. CIF files can be obtained from the Cambridge Crystallographic Data Centre, Cambridge, UK with the REF codes 2010164. The crystal structure analysis for cocrystal was performed to identify the molecular interactions between BCl·$2H_2O$ and LA. The 1:1:1 cocrystal hydrate adopts the triclinic P-1 space group. And there is no proton transfer occurred from LA to BCl molecule, which indicated BCl-LA-H_2O is a salt-cocrystal. The asymmetric unit of BCl-LA-H_2O contains one BCl, one SA, and one water molecule (Fig. 2a), they are linked through C6-H6A···Cl_1, O8-H8A···Cl_1, C19-H19···Cl_1, O6-H6···O8, and C16-H16···O5 to form a chain (Fig. 2b). The adjacent chains are further linked by C11-H11A···O7 to generate a sheet. The adjacent sheets are further connected by intersheet hydrogen bonds to form the three-dimensional (3D) structure of BCl-LA-H_2O (Fig. 2c).

Table 1: Crystallographic data of BCl-LA-H_2O

	BCl-LA-H_2O
Empirical formula	$C_{23}H_{26}ClNO_8$
Formula weight	479
Temperature/K	173.0
Crystal system	Triclinic
Space group	P-1(2)
a/Å	7.4087(11)
b/Å	11.9693(17)
c/Å	13.830(2)
α/°	70.047
β/°	74.868
γ/°	84.194
Volume/Å^3	1112.72(30)
Z	2

Table 2: Hydrogen bonding distances and angles of BCl-LA-H_2O

Hydrogen bond	D-H(Å)	H···A(Å)	D···A(Å)	<D-H···A(°)
C6-H6A···Cl$_1$	0.991	2.826	3.793	165.01
O8-H8A···Cl$_1$	0.850	2.269	3.120	178.73
C19-H19···Cl$_1$	0.950	2.791	3.565	139.31
O6-H6···O8	0.840	1.780	2.604	166.51
C16-H16···O5	0.950	2.456	3.289	146.29
C11-H11A···O7	0.990	2.524	3.493	165.94
C6-H6B···C18	0.990	2.761	3.217	145.02

2.2. PXRD analysis

PXRD patterns of BCl·2H_2O, calculated BCl-LA-H_2O from single crystal data, and BCl-LA-H_2O cocrystal prepared by the liquid-assisted grinding are shown in Fig. 3. There is no experimental PXRD pattern of LA. This is because LA is a liquid at room temperature, which makes its PXRD is impossible to be provided. For the BCl·2H_2O and BCl-LA- H_2O systems, the characteristic diffraction peaks were identified as follows: BCl·2H_2O 2θ = 8.64°, 9.09°, 12.98°, 16.31°, 25.40°, 26.26°, and 26.86°; BCl-LA-H_2O 2θ = 8.43°, 14.82°, 15.26°, 18.86°, 19.99°, 24.93°, and 25.71°. The cocrystal showed different and unique diffraction peaks at 2θ values from API, indicating the formation of a new crystalline phase.

2.3. Thermal analysis

The TGA and DSC curves of BCl·2H_2O and BCl-LA-H_2O cocrystal were presented in Fig. 4. The TGA curve of BCl·2H_2O showed the first weight loss of 8.9% occur in the temperature range from 30 to 100°C, which is close to the theoretical content (8.8%) of two water molecules. As viewed from the Fig. 4b, the thermal profiles of BCl·H_2O revealed an endothermic peak at 87.3°C, which is due to the dehydration event. There was a sharp endothermic peak at 193.5°C attributed to melting. From room temperature to 100°C, the TGA curves of BCl-LA-2H_2O showed weight loss of nearly 8.6%. And there is an endothermic peak at the corresponding temperature, which indicating that BCl-LA-H_2O is combined with water molecules. According to the results of SCXRD analysis (Fig. 2), which indicating that BCl-LA-H_2O is monohydrate. Therefore, the cocrystal combines one molecule of water (3.8%) and some adsorbed water. The DSC curve of BCl-LA-2H_2O exhibited an endothermic peak at 217°C which is due to the melting. The generation of new solid form were inferred from the apparently different thermal behavior. It is worth noting that, the melting point of cocrystal is higher compared with the starting components. The increase of degradation temperature further indicated that the formation of cocrystal can improve the thermal stability of API.

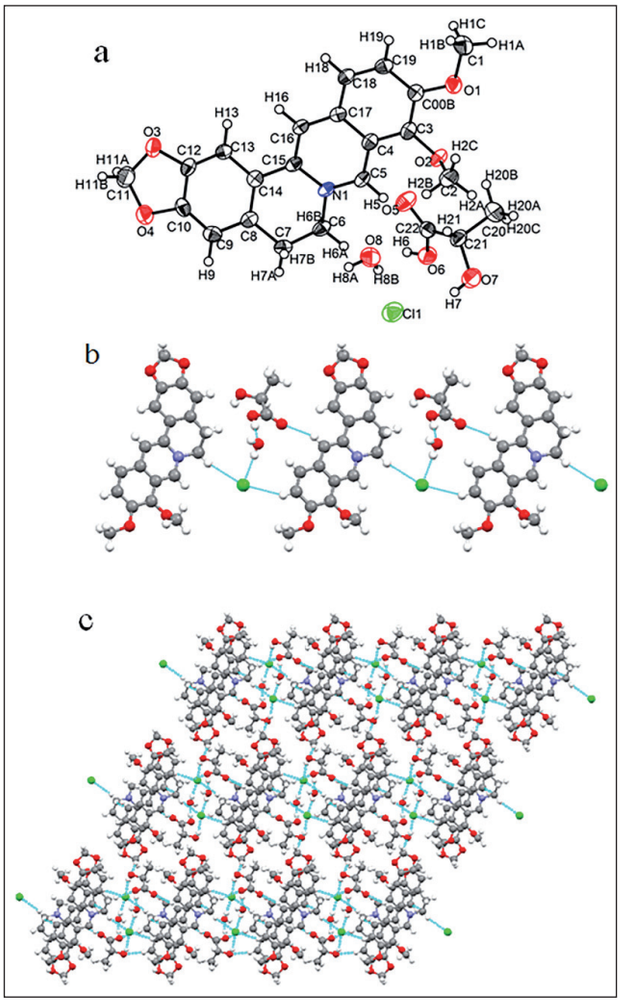

Fig. 2: The crystal structures of BCl-LA-H_2O, (a) thermal ellipsoid drawing including atomic labelling scheme, (b) key intermolecular interactions (hydrogen bonds are teal colored), (c) molecular packing.

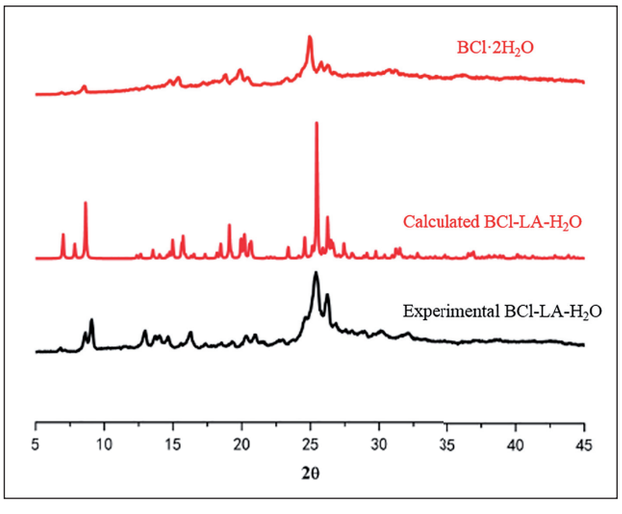

Fig. 3: The PXRD patterns of BCl·2H_2O, the calculated BCl-LA-H_2O, and the experimental BCl-LA-H_2O.

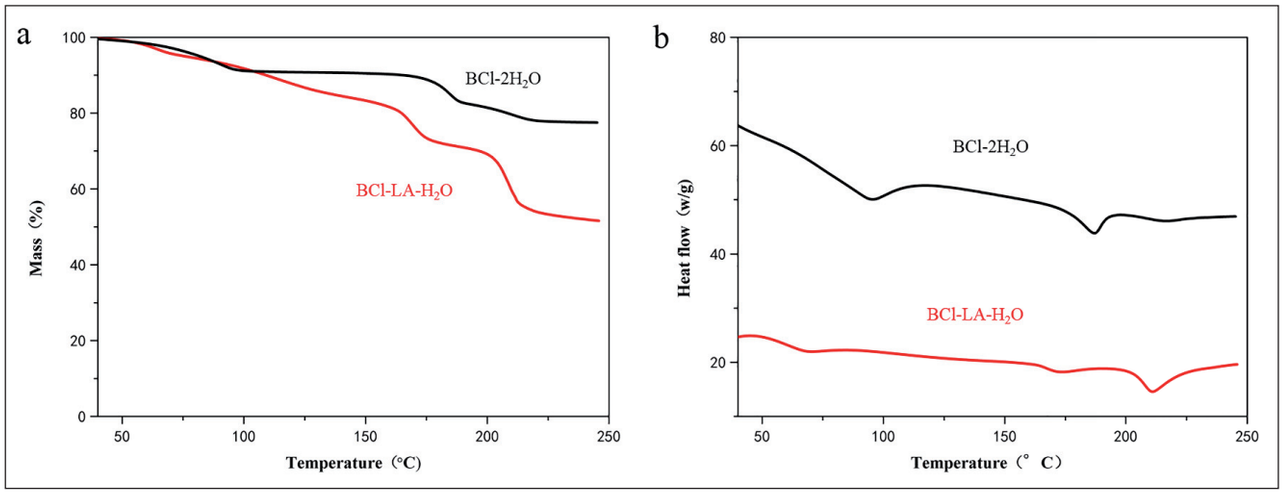

Fig. 4: Thermal properties of BCl·2H_2O and BCl-LA-H_2O, (a) TGA and (b) DSC

2.4. FTIR analysis

The FTIR spectra for BCl·2H_2O and BCl-LA-H_2O were presented to further confirm the intermolecular interactions between BCl·2H_2O and LA, which can be identified by the changes in vibrational frequencies of corresponding functional groups (Fig. 5). Analysis of the spectrum of BCl·2H_2O showed distinctive bands at 3421, 1621, and 1504 cm^{-1}, which respectively represent O-H, C=C, and O-CH_3 stretching frequency. In the BCl-LA-H_2O cocrystal, the O-H stretching frequency of BCl·2H_2O demonstrated a red shift (3421 cm^{-1}→3301cm^{-1}), C=C frequency shifted to 1617 cm^{-1}, and O-CH_3 frequency shifted to 1493 cm^{-1}. Among these, there is a strong O-H peak at 3301 cm^{-1}, which indicated that water molecules are still present in the cocrystal. This result is consistent in SCXRD analysis. These changes in wavenumbers indicated that these functional groups are involved in the formation of the hydrogen bond in the cocrystal. It also further indicated formation of new phase.

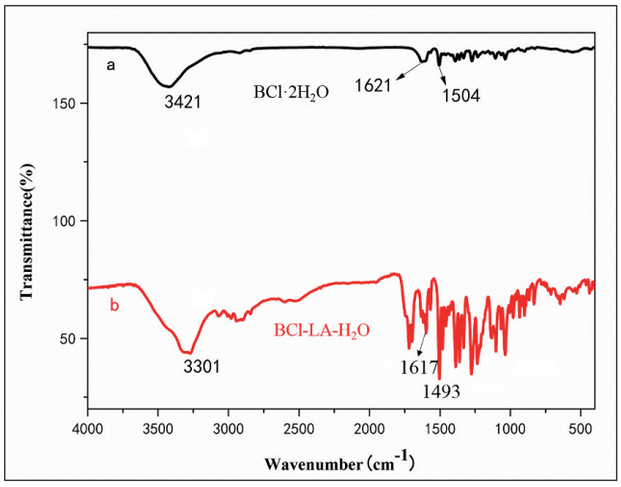

Fig. 5: FTIR spectra of (a) BCl·2H_2O, (b) BCl-LA-H_2O.

2.5. Solubility

The solubility data of BCl·2H_2O and BCl-LA-H_2O in these selected solvents (water, methanol, and ethanol) were presented in Table 3 and Table 4. The results showed that solubility was improved with the increasing temperature. And at 25°C and 37°C, the decreasing order of solubility of BCl·2H_2O and BCl-LA-H_2O cocrystal in the different solvents was methanol > water > ethanol. In addition, the solubility of BCl- LA-H_2O is better than BCl·2H_2O in all three solvents at the same temperature.

Table 3: Solubility data of BCl·2H_2O and BCl-LA-H_2O at 25°C (mg/ml)

	Water	Methanol	Ethanol
BCl·2H_2O	8.714	20.503	3.221
BCl-LA-H_2O	8.756	21.962	3.410

Table 4: Solubility data of BCl·2H_2O and BCl-LA-H_2O at 37°C (mg/ml)

	Water	Ethanol	Methanol
BCl·2H_2O	14.105	4.742	27.956
BCl-LA-H_2O	14.417	5.219	34.558

2.6. Dissolution

Dissolution is an important characteristic that is related to bioavailability. The dissolution profiles of BCl·2H_2O and BCl-LA-H_2O were presented in Fig. 6. As observed from the dissolution profiles, the areas under curve for BCl·2H_2O and BCl-LA-2H_2O are 10908 ± 194 and 11469.48±172 mg·min, respectively. The time of cocrystal reached dissolution balance used for BCl-LA-H_2O is 25min, and the BCl·2H_2O is 90min. It is obvious that the cocrystallization formation results in an improvement of dissolution in this case.

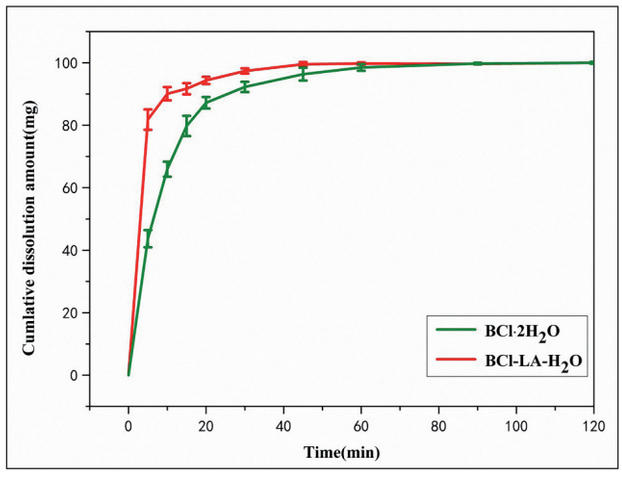

Fig. 6: Dissolution profiles of BCl·2H_2O and BCl-LA-H_2O at 37 °C (n= 3).

2.7. Dynamic vapor sorption

The DVS isotherms of BCl·2H_2O and BCl-LA-H_2O cocrytsal were presented in Fig. 7. At low humidity (0-10% RH), BCl rapidly absorbed water with the increasing of relative humidity, and gradually transformed to dihydrate. According to the measured amount of adsorbed water in the BCL sample (8.8%), the increase of water absorption is attributed to the phase transition from BCL to dihydrate. It can be stable in the range of nearly 20% RH -70% RH. And the sample absorbed a significant amount of water at 70-95% RH and gradually transformed to tetrahydrate. During the desorption process, tetrahydrate is very stable from 95% RH to 20% RH, then it lost approximately 16% of water which is equal to four H_2O molecules in mass at 20-0% RH.

In the range of 0-10% RH, the BCl-LA-H_2O gains almost no moisture (0.3% of water). Then it remained stable in the range of nearly 20% -70% RH. It absorbed about two H_2O molecular at 70-95% RH. During desorption process, BCl-LA-H_2O lost three H_2O molecules from 95% RH to 0% RH slowly. Compared with BCl·2H_2O, BCl-LA-H_2O cocrystal exhibits lower hygroscopicity, which improves the problem of phase transition in the process of wet granulation due to strong hygroscopicity.

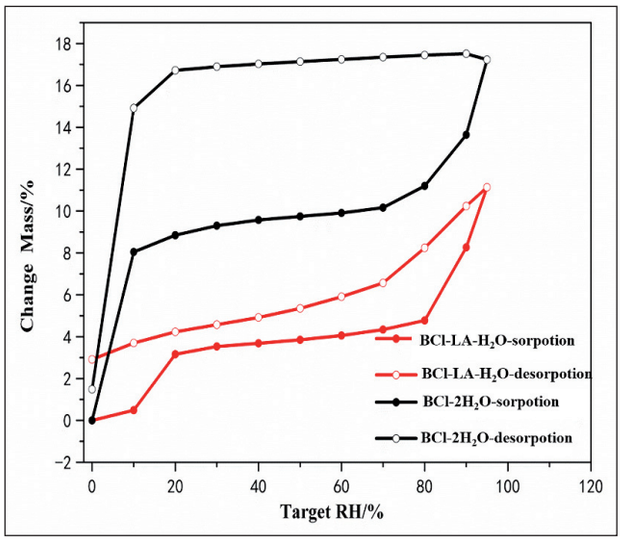

Fig. 7: DVS isotherms of BCl·2H_2O and BCl-CA-H_2O (open symbols for desorption and solid symbols for sorption).

2.8. Conclusions

In this study, LA was employed as a coformer to obtain cocrystal with BCl·2H_2O by liquid-assisted grinding method. The structure of the novel cocrystal was determined by single crystal X-ray diffraction analysis. The result showed that there is no proton transfer occurred from LA to BCl molecule, which indicated BCl-LA-H_2O is a salt-cocrystal. Compared with BCl·2H_2O, BCl-LA-H_2O exhibited significantly increasing performance in solubility, dissolution, and hygroscopicity. Specially, a lower hygroscopicity of BCl-LA-H_2O, which improved the solid-state instability of BCl·2H_2O in pharmaceutical process. Moreover, the melting point of cocrystal was higher than the starting components, which indicated the formation of cocrystal can improve the thermal stability of API. Overall, these results reinforce that the cocrystal can be a promising API candidate.

3. Experimental

3.1. Materials

Berberine hydrochloride (BCl, 98% purity) was purchased from Shanghai Civi Chemical Co., Ltd (Shanghai, China), L (+)-lactic acid (LA, 99.4% purity) was purchased from Aladdin Industrial Corporation (Shanghai, China). Solvents were used without any further purification. And water used was double-distilled.

3.2. Methods

3.2.1. Preparation of BCl-LA cocrystal hydrate (1:1:1)

A mixture of BCl·2H_2O (408 mg, 1mmol) and LA (90 mg, 1mmol) were dipped together in a molar ratio of 1:1 and milled in agate mortar for an hour at room temperature. During this procedure, 1~2 drops of ethanol were added to the mixed powder.

3.2.2. Preparation of single crystal

A mixture of BCl·2H_2O and LA (300mg, molar ratio 1:1) was stirred in 10 mL of methanol for 24 h. It was then filtered and the clear solution was allowed to evaporate slowly at room temperature in a parafilm sealed glass vial. Then the pale yellow single crystals could be obtained in 2 days (Fig. 8), from which suitable crystals were chosen for SCXRD measurements.

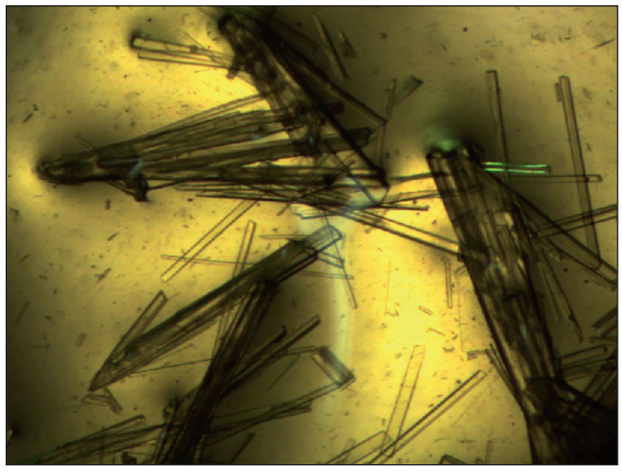

Fig. 8: Image of single crystals under the microscope.

3.2.3. Single crystal x-ray diffraction (SCXRD)

The data were selected on a Bruker APEX-II diffractometer with Mo-Kα radiation sealed tube source at 173.0 K. The structure was solved by direct methods using SHELXS and refined on F^2 by full-matrix least-squares methods using the SHELX program package. Non-hydrogen atoms were refined anisotropically, and organic hydrogen atoms were generated geometrically. Fixed hydrogen and carbon atoms in geometrically constrained positions. The hydrogen atoms were included in the position associated with the oxygen atoms and the nitrogen atoms.

3.2.4. Powder x-ray diffraction (PXRD)

The PXRD patterns were obtained in a D2 Advance powder diffractometer pattern (D2-phase, BRUKER, Germany) using Cu Kα radiation source over an angular range of 5–40° (2θ) with a step size of 0.014° and a step time of 0.1 s. The current and voltage were set 10 mA and 30 kV, respectively. The Mercury 3.7 software was used to generate the calculated PXRD pattern.

3.2.5. Differential scanning calorimetry (DSC)

About 5-10 mg of samples were placed into a sample holder using a SDTQ 600 Instrument and heated from room temperature to 250 °C at a rate of 10°C/min with nitrogen flowing at 50mL/min.

3.2.6. Thermogravimetric (TG) analysis

TG analysis was performed in a nitrogen atmosphere using SDTQ 600 Instrument. About 5-10 mg of samples were placed into a sample holder and heated from room temperature to 250 °C at a rate of 10 °C/min.

3.2.7. Fourier transform infrared spectroscopy (FTIR)

FTIR spectra were obtained by a Bruker EQUINOX 55 FT-IR spectrometer using the KBr pellet technique to further confirm the cocrystal formation. The samples and KBr were mixed and dried and the particle size was less than 2 hum and pressed into the mould. Then the data was recorded by its absorption of infrared radiation over the region from 4000cm^{-1} to 400 cm^{-1} for 64 scans.

3.2.8. High performance liquid chromatography (HPLC) assay

HPLC analysis was performed for content determination in the dissolution and solubility measurement. The contents of BCl and BCl-LA-H_2O were determined using an Agilent LC-1260S system. Separation was achieved using a C18 column

(4.6mm×150mm, 5μm) and detected at 230 nm. The mobile phase consisted of methanol and 0.4% (v/v) phosphoric acid solution, which was started with 5% (v/v) methanol (4min), followed by an immediate jump to 60% (v/v) methanol (20min), and returned immediately to 5% (v/v) methanol (21min), and then kept at 5% (v/v) methanol (30 min). The flow was run at 1.0 mL/min, and the sample injection volume was 10 μL. And the column temperature was set at 30 °C. The response linearity was ensured by linear determination factors R^2, which was 1. The concentration of BCl in the range of 0.01966-0.5898mg/ml has good linear relationship.

3.2.9. Solubility determination

API and BCl-LA-H_2O were measured in distilled water, ethanol and methanol according to shake-flask method at 25°C and 37°C. Specifically, 200 mg of samples were added to 10 mL of these solvents in vials, and stirred for 24 hours to prepare super-saturated solution. The samples were then filtered through 0.22μm nylon filter and the filtrate was diluted to appropriate concentration for HPLC analysis. Solubility measurements were carried out in triplicate.

3.2.10. Powder dissolution experiments

The powders were milled to powders and sieved using a 100 mesh sieve. 100mg of API and 129mg of BCl-LA-H_2O cocrystal were dipped into 900ml water at 37°C respectively, with the paddle rotating at 50 rpm. Sampling was carried out at 5, 10, 15, 20, 30, 45, 60, 90 and 120 min, 5 mL of the dissolution medium was withdrawn and immediately replaced with 5 mL of fresh medium. After filtration through 0.22μm nylon filters, the amount of dissolved BCl was determined using the HPLC method. Dissolution test was repeated three times.

3.2.11. Dynamic vapor sorption (DVS) study

The DVS experiments were carried out on a DVS instrument (Surface Measurement Systems, UK) at 25 ± 0.1 °C. Then, BCl·$2H_2O$ and BCl-LA-H_2O were exposed to a series of relative humidity (RH) from 0%-95%-0% RH with a step size of 10% RH. Finally, the adsorption/desorption isotherms were calculated from the equilibrium mass values.

Acknowledgments: This study was financially supported by Postgraduate Research and Innovation Project of Shanghai University of Engineering Science (20KY0410), and the CAMS Initiative for Innovative Medicine (2016-I2M-1-011).

Conflict of interests: The authors declare no competing financial interest.

References

Bavishi DD, Borkhataria CH (2016) Spring and parachute: how cocrystals enhance solubility. Prog Cryst Growth Charact Mater 62: 1-8.

Chen Y, Li L, Yao J, Ma YY, Chen JM, Lu TB (2016) Improving the solubility and bioavailability of apixaban via apixaban–oxalic acid cocrystal. Cryst Growth Des 16: 2923-2930.

Childs SL, Chyall LJ, Dunlap JT, Smolenskaya VN, Stahly BC, Stahly GP (2004) Crystal engineering approach to forming cocrystals of amine hydrochlorides with organic acids. Molecular complexes of fluoxetine hydrochloride with benzoic, succinic, and fumaric acids. J Am Chem Soc 126: 13335-13342.

Childs SL, Kandi P, Lingireddy SR (2013) Formulation of a danazol cocrystal with controlled supersaturation plays an essential role in improving bioavailability. Mol Pharm 10: 3112-3127.

Desiraju GR (2013) Crystal engineering: from molecule to crystal. J Am Chem Soc 135: 9952-9967.

Du Y, Cai Q, Xue J, Zhang Q, Qin D (2017) Structural investigation of the cocrystal formed between 5-fluorocytosine and fumaric acid based on vibrational spectroscopic technique. Spectrochim Acta Part A 178: 251-257.

Jin Y, Khadka DB, Cho WJ (2015) Pharmacological effects of berberine and its derivatives: a patent update. Expert Opin Ther Pat 26: 229-243.

Jung MS, Kim JS, Kim MS, Alhalaweh A, Cho W, Hwang SJ, Velaga SP (2010) Bioavailability of indomethacin: accharin cocrystals. J Pharm Pharmaco 62: 1560-1568.

Kobayashi Y, Ito S, Itai S, Yamamoto K (2000) Physicochemical properties and bioavailability of carbamazepine polymorphs and dihydrate. Int J Pharm 193: 137-146.

Liu CS, Zheng YR, Zhang YF, Long XY (2016) Research progress on berberine with a special focus on its oral bioavailability. Fitoterapia 108: 274-282.

Lu Q, Dun J, Chen J, Liu S, Sun CC (2019) Improving solid-state properties of berberine chloride through forming a salt cocrystal with citric acid. Int J Pharm 554: 14-20.

Pingali S, Donahue JP, Payton-Stewart F (2015) Tetrahydroberberine, a pharmacologically active naturally occurring alkaloid. Acta Crystallog Sect C: Struct Chem 71: 262-265.

Qiao N, Li M, Schlindwein W, Malek N, Davies A, Trappitt G. (2011) Pharmaceutical cocrystals: an overview. Int J Pharm 419: 1-11.

Su J, Zhang R, Lian Y, Kamal Z, Cheng Z, Qiu Y, Qiu M (2019) Preparation and characterization of erythrocyte membrane-camouflaged berberine hydrochloride-loaded gelatin nanoparticles. Pharmaceutics 11: 93.

Sun Y, Xun K, Wang Y, Chen X (2009) A systematic review of the anticancer properties of berberine, a natural product from Chinese herbs. Anti-Cancer Drugs 20: 757-769.

Shimpi MR, Alhayali A, Cavanagh KL, Rodríguez-Hornedo N, Velaga SP (2018) Tadalafil–malonic acid cocrystal: physicochemical characterization, pH-solubility, and supersaturation studies. Cryst Growth Des 18: 4378-4387.

Tong HH, Chow AS, Chan H, Chow AH, Wan YK, Williams ID, Shek FL, Chan CK (2010) Process-induced phase transformation of berberine chloride hydrates. J Pharm Sci 99: 1942–1954.

Thakuria R, Delori A, Jones W, Lipert MP, Roy L, Rodríguez-Hornedo N (2013) Pharmaceutical cocrystals and poorly soluble drugs. Int J Pharm 453: 101-125.

Xu H, Liu C, Huang C, Chen L, Zheng Y, Huang S, Long X (2019) Nanoemulsion improves hypoglycemic efficacy of berberine by overcoming its gastrointestinal challenge. Colloids Surf B 181: 927-934.

Zhu JX, Tang D, Feng L, Zheng ZG, Wang RS, Wu AG, Duan TT, He B, Zhu Q (2013) Development of selfmicroemulsifying drug delivery system for oral bioavailability enhancement of berberine hydrochloride. Drug Dev Ind Pharm 39: 499-506.